Quantitative trait loci that determine lipoprotein cholesterol levels in DBA/2J and CAST/Ei inbred mice[1,2]

Malcolm A. Lyons,* Henning Wittenburg,*,† Renhua Li,* Kenneth A. Walsh,* Gary A. Churchill,* Martin C. Carey,† and Beverly Paigen[3,*]

The Jackson Laboratory,* Bar Harbor, ME 04609; and Department of Medicine,† Harvard Medical School, Division of Gastroenterology, Brigham and Women's Hospital and Harvard Digestive Diseases Center, Boston, MA 02115

Abstract **To investigate genetic contributions to individual variations of lipoprotein cholesterol concentrations, we performed quantitative trait locus/loci (QTL) analyses of an intercross of CAST/Ei and DBA/2J inbred mouse strains after feeding a high-cholesterol cholic acid diet for 10 weeks. In total, we identified four QTL for HDL cholesterol. Three of these were novel and were named *Hdlq10* [20 centimorgans (cM), chromosome 4], *Hdlq11* (48 cM, chromosome 6), and *Hdlq12* (68 cM, chromosome 6). The fourth QTL, *Hdl1* (48 cM, chromosome 2), confirmed a locus discovered previously using a breeding cross that employed different inbred mouse strains. In addition, we identified one novel QTL for total and non-HDL cholesterol (8 cM, chromosome 9) that we named *Chol6*. *Hdlq10*, colocalized with a mutagenesis-induced point mutation (*Lch*), also affecting HDL.** **We provide molecular evidence for *Abca1* as the gene underlying *Hdlq10* and *Ldlr* as the gene underlying *Chol6* that, coupled with evidence generated by other researchers using knockout and transgenic models, causes us to postulate that polymorphisms of these genes, different from the mutations leading to Tangier's disease and familial hypercholesterolemia, respectively, are likely primary genetic determinants of quantitative variation of lipoprotein levels in mice and, by orthology, in the human population.**—Lyons, M. A., H. Wittenburg, R. Li, K. A. Walsh, G. A. Churchill, M. C. Carey, and B. Paigen. **Quantitative trait loci that determine lipoprotein cholesterol levels in DBA/2J and CAST/Ei inbred mice.** ***J. Lipid Res.*** **2003.** 44: **953–967.**

Supplementary key words *Castaneus* • mouse • nuclear receptor • high density lipoprotein • low density lipoprotein • intercross • *Abca1* • *Ldlr* • *Pparg*

HDL levels are correlated inversely with atherosclerosis (1) and are also associated negatively with cholesterol gallstones (2). HDL is associated closely with "reverse cholesterol transport," a term often simultaneously applied to macrophage cholesterol efflux and centripetal cholesterol flux, which refers to the movement of cholesterol from periphery to the liver for elimination (3). However, recent investigations with mice revealed that centripetal cholesterol flux is not determined by the absolute concentration of plasma HDL (4–6), findings that are supported by human studies (7). Nonetheless, HDL is involved in the elimination of excess peripheral cholesterol from the body, and HDL-mediated macrophage cholesterol efflux remains as the crucial determinant of foam cell formation and atherogenesis (3, 8, 9). Patients with Tangier's disease (mutant or absent ABCA1) who possess severely diminished HDL concentrations and display premature atherosclerosis (10, 11) dramatically highlight this fact. Furthermore, HDL exhibits many other antiatherogenic effects (12, 13). On the other hand, LDL cholesterol concentrations are correlated directly with atherosclerosis (14). These crucial roles in the development of atherosclerosis render the pathophysiological and genetic background of variation in individual lipoprotein levels an extremely important field of investigation, both from a clinical and a public health perspective.

In addition to mutations in *ABCA1*, monogenic HDL deficiency can be caused by mutations in *APOA1*, *LCAT*, and *LPL* (15). To date, five disorders of LDL metabolism with monogenic inheritance have been identified as stemming from mutations in *LDLR*: *APOB*, *ARH*, *ABCG5*, and/or *ABCG8* (16), and *CYP7A1* (17). These disorders of lipoprotein metabolism are rare but shed light on important mechanisms of lipid metabolism. It is unclear whether it is

Manuscript received 2 January 2003 and in revised form 10 February 2003.

Published, JLR Papers in Press, February 16, 2003.
DOI 10.1194/jlr.M300002-JLR200

Abbreviations: CAST, CAST/Ei; D2, DBA/2J; LOD, logarithm of the odds ratio; QTL, quantitative trait locus/loci; SNP, single nucleotide polymorphism; SSLP, simple sequence-length polymorphism.

[1] This paper was presented in part at the Digestive Diseases Week 2002, San Francisco, and published in abstract form in *Gastroenterology*. 2002. **122:** A626.

[2] DNA sequences cited in this manuscript have been submitted to GenBank with the following accession numbers: *Nr1h3*, AY195870, CAST/Ei; AY195871, DBA/2J; *Pparg*, AY208183, CAST/Ei; and AY208184, DBA/2J.

[3] To whom correspondence should be addressed.
e-mail: bjp@jax.org

polymorphisms of these same genes that account for the monogenic disorders of lipid metabolism or polymorphisms of different genes that are responsible for the variation of plasma cholesterol levels in the general population. Variations among individual lipoprotein concentrations in the general population are determined by a complicated genetic basis involving multiple genes and gene-gene, as well as gene-environment, interactions (18). Therefore, lipoprotein cholesterol levels are one example of a complex trait. Others include many common diseases, such as atherosclerosis, hypertension, diabetes, and asthma. Revealing the mechanisms of the common complex diseases is among our greatest challenges and will contribute greatly to health (19).

A powerful approach to localizing and identifying genes underlying complex traits is to employ quantitative trait locus/loci (QTL) analysis using murine breeding crosses (20, 21). Our laboratory has utilized QTL analysis to investigate the genetics underlying cholesterol gallstone formation, atherosclerosis, and lipoprotein metabolism (18, 21–23). We report here the results of our investigation of plasma HDL, total HDL, and non-HDL cholesterol concentrations after feeding F_2 progeny a lithogenic (i.e., promoting cholesterol gallstone formation)/atherogenic diet containing high amounts of cholesterol and the hydrophobic bile acid cholic acid, which promotes cholesterol absorption and "humanizes" both the bile salt pool and lipoprotein profile. Gallstone susceptibility loci detected with this intercross are reported elsewhere (24). Primarily, our aim was not only to identify novel loci but also to confirm previously identified loci, thus establishing the validity of a QTL across a variety of inbred strains. We detected five QTL in total; four were associated with HDL cholesterol, whereas the fifth encompassed total and non-HDL cholesterol levels. We provide molecular evidence for a single candidate gene (*Abca1*) underlying the QTL for HDL cholesterol on chromosome 4 (*Hdlq10*), and a single candidate gene (*Ldlr*) underlying the QTL for total/non-HDL cholesterol on chromosome 9 (*Chol6*). These data, coupled with evidence generated by other researchers using knockout and transgenic models, cause us to postulate that polymorphisms of these genes, different from the mutations leading to Tangier's disease and familial hypercholesterolemia, respectively, are likely to be primary genetic determinants of quantitative variation of lipoprotein levels in mice and, by orthology, in the human population.

MATERIALS AND METHODS

Animals and diet

CAST/Ei (CAST) and DBA/2J (D2) mice were obtained from the breeding facilities of The Jackson Laboratory (Bar Harbor, ME). Reciprocal F_1 progeny [i.e., (CAST × D2)F_1 derived from female CAST × male D2 and (D2 × CAST)F_1 derived from female D2 × male CAST] and F_2 progeny, derived from both lineages, were bred and maintained at The Jackson Laboratory. Animals were housed in a temperature-controlled room (22–23°C) under a 14 h light-10 h dark cycle. Breeding pairs were fed low-cholesterol (<0.02%) chow (Purina 5001; PMI Feeds, Richmond, IL), as were experimental animals, until they reached 6–8 weeks. At that time, mice were transferred to the lithogenic diet (identical to atherogenic diet) comprising, by weight, butter fat (15%), cholesterol (1%), cholic acid (0.5%), corn oil (2%), sucrose (50%), casein (20%), and essential minerals and vitamins (22). Male mice only were used in this study and had free access to food and water. The Institutional Animal Care and Use Committees of The Jackson Laboratory and Harvard University approved all experimental protocols.

Phenotyping

Animals were fasted 4 h prior to collection of blood via the retro-orbital sinus. EDTA (2 μmol per tube) was used as an anticoagulant. Blood was maintained at 4°C until plasma was isolated by centrifugation (10,000 *g*, 5 min) and was stored at −20°C until analysis. HDL and total cholesterol were analyzed using an automated chemistry analyzer and the manufacturer's reagents (Synchron CX-5 Delta, Beckman, Palo Alto, CA) based on the cholesterol esterase and cholesterol oxidase reactions (25, 26). HDL cholesterol was measured after Mg^{2+}-dextran sulfate proteoglycan precipitation of apolipoprotein B (apoB)-containing particles (27). Total cholesterol was generally measured diluted 2-fold with phosphate buffered saline. Because mice were fasted before blood was collected and because chylomicrons display very short half-lives (28), non-HDL was presumed to comprise predominantly VLDL and LDL. Non-HDL was calculated as the difference between total and HDL cholesterol concentrations.

Genotyping

DNA was prepared from tail samples using phenol-chloroform extraction subsequent to Proteinase K (Fisher Scientific, Medford, MA) digestion and were resuspended in water. Standard PCR amplification of simple sequence-length polymorphisms (SSLPs; n = 109; **Fig. 1**) that discriminate between CAST and D2 alleles (MapPairs primers, Research Genetics, Huntsville, AL) was used to genotype F_2 progeny (except Y chromosome) using both gel electrophoresis (4% agarose, NuSieve 3:1, FMC BioProducts, Rockland, ME) and capillary electrophoresis (ABI 3700 Sequence Detection System, Applied Biosystems, Foster City, CA). Reported genetic map positions were retrieved from the Mouse Genome Database (http://www.informatics.jax.org).

QTL analyses

To identify single and interacting QTL associated with lipoprotein cholesterol concentrations, the three-stage analysis of Sen and Churchill (29, 30) was employed. Single loci associated with the traits were detected by interval mapping. Significance thresholds were determined by permutation testing (31), and 95% confidence intervals were calculated as described (29). A multiple imputation algorithm was used to account for missing marker genotypes (29). To account for possible lineage effects of the QTL, lineage was included in the analysis as an additive covariant. Results are expressed as logarithm of the odds ratio (LOD) scores, the traditional measure of linkage (20). In the second stage, QTL that affected the trait by interacting with one another were sought using a genome-wide simultaneous search for gene pairs (30). In the third stage, a multiple regression analysis was performed that integrated the single and interacting loci identified in the first two stages to determine the contribution of each QTL in combination with all other QTL (30). The software is available at http://www.jax.org/research/churchill.

mRNA expression analyses

In the parental strains of mice, CAST and D2, and in selected F_2 progeny, hepatic levels of mRNA expression were determined for genes that colocalized with QTL and were known to have a

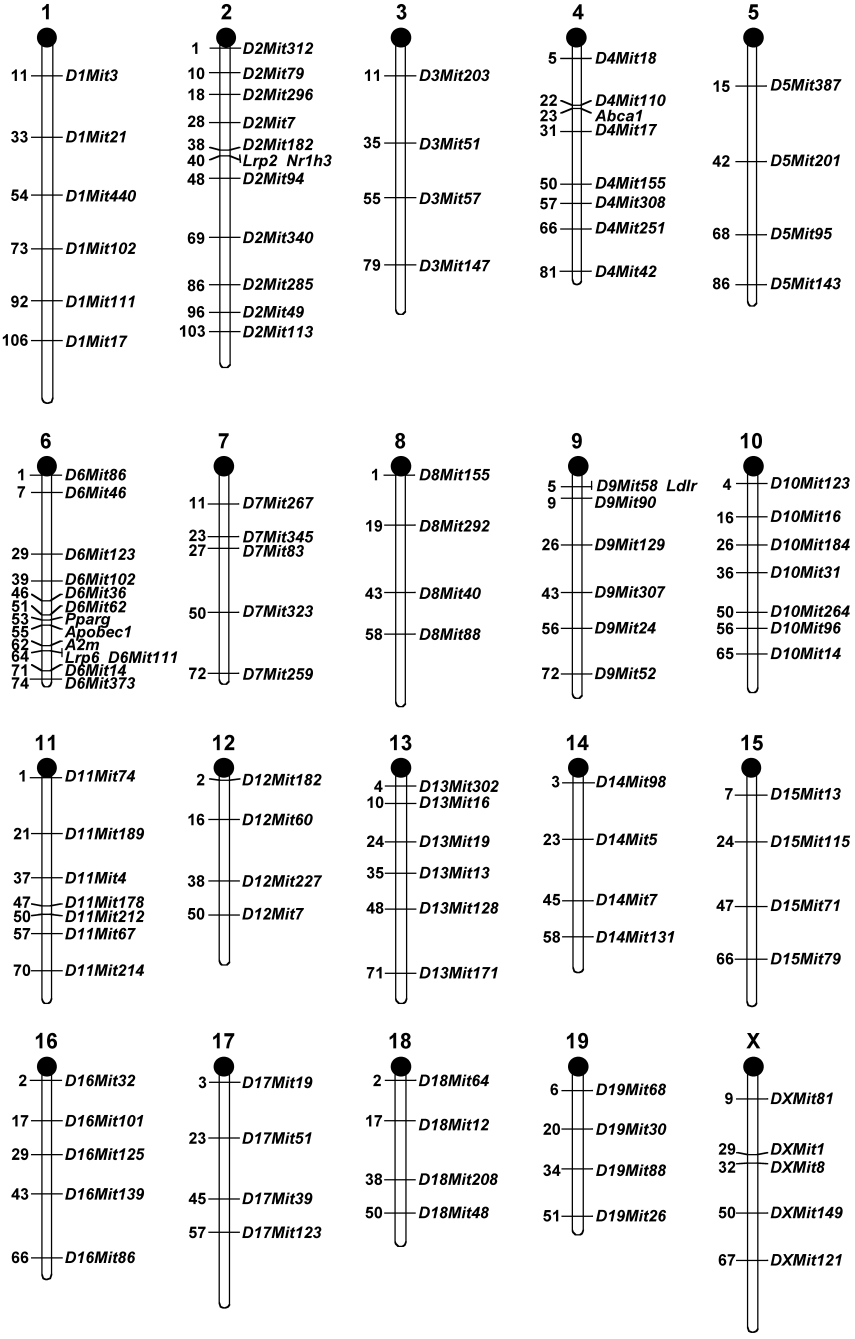

Fig. 1. Chromosomal map indicating the genetic positions of simple sequence-length polymorphism (SSLP) markers used for quantitative trait locus/loci (QTL) analyses and positional candidate genes. In total, 109 SSLPs covering the 19 autosomes and chromosome X were used to genotype 278 male mice using a combination of gel and capillary electrophoresis. The chromosome number is indicated at the top of the chromosome. The genetic map positions are given in centimorgans (cM) on the left of the chromosomes and were retrieved from the Mouse Genome Database (http://www.informatics.jax.org). The SSLP names and positional candidate gene names are given on the right of the chromosomes.

direct or indirect role in lipid metabolism (positional candidate genes). To collect hepatic tissue for mRNA expression analyses, mice of the parental strains (five per strain) were fed the lithogenic diet for 4 weeks, assuming a steady state for the expression of genes induced by the diet. After that period, food was taken away from the animals at 6 AM (1 h into light cycle). Starting at 10 AM, animals were sacrificed by cervical dislocation and then subjected to transcardiac perfusion via the left ventricle with ice-cold phosphate-buffered saline. This procedure was conducted on alternate CAST and D2 mice to minimize any possible effect of diurnal variation or length of fasting. Livers of F_2 animals were harvested at the time of sacrifice after fasting 4 h, but did not undergo perfusion. They were frozen in liquid nitrogen and stored at −80°C until analysis. For expression analyses, groups of F_2 animals were selected based on their genotypes at the QTL peaks and the SSLPs flanking those peaks. At each of the QTL

linked to *D2Mit94*, *D4Mit110*, and *D9Mit58*, 10 animals per genotype per locus were selected, whereas at the QTL linked to *D6Mit36* and *D6Mit14*, 15 animals were selected per genotype.

Total RNA was isolated from liver using a commercially available kit (RNeasy Mini Kit, QIAGEN, Valencia, CA) according to the manufacturer's instructions. First-strand cDNA was reverse transcribed (2 μg RNA, 20 μl final volume per reaction) with a commercially available kit (Omniscript Reverse Transcription Kit, QIAGEN) using a combination of oligo deoxythymidine [$(dT)_{15}$, 500 ng per reaction, Promega, Madison, WI] and random hexamers (250 ng per reaction, Invitrogen, Carlsbad, CA). Quantitative kinetic (real-time) PCR was performed with an ABI 7700 or 7900 Sequence Detection System using a SYBR Green PCR Mastermix (Quantitect SYBR Green PCR Mastermix, QIAGEN); expression of *Gapd* served as internal standard. Gene-specific oligonucleotide primers (100 nM final concentration) were designed using Primer3 software (http://www-genome.wi.mit.edu/cgi-bin/primer/primer3_www.cgi) and are defined in **Table 1**. A 10-fold dilution of cDNA (2 μl per reaction) was used for real-time PCR reactions. Because the internal control (*Gapd*) was more abundant than the target genes, it reached the critical cycle-threshold (C_t) sooner. Therefore, we calculated Ct^{Gapd}-Ct^{Target} to yield ΔC_t, the number of cycles in excess of *Gapd* fluorescence required to reach *Target* fluorescence (usually a negative number in these experiments). Because PCR doubles the number of target DNA molecules per cycle, $2^{\Delta Ct}$ describes the relative deficit of *Target* molecules compared with *Gapd* molecules. Hence, we normalized the resultant figures and expressed them per 10^6 molecules of *Gapd*. Statistical analyses were performed on the normalized data.

DNA sequencing

Real-time PCR products were subjected to gel (2.5%) electrophoresis with ethidium bromide staining or dissociation analysis using the real-time PCR machine to ensure specific amplification of a single product. Direct DNA sequencing of the amplicon followed by genomic DNA database interrogation (BLAST using ENSEMBL database) was employed to confirm the authenticity of real-time PCR amplification products. The cDNA and ~750 nucleotides proximal to the transcription start site of *Nr1h3*, one of the key candidate genes for the chromosome 2 QTL, were sequenced to investigate putative polymorphisms that may determine mRNA expression differences and the existence of potential amino acid substitutions. Direct sequencing was performed on overlapping PCR amplification products using Big Dye Terminator Cycle Sequencing Chemistry and the ABI 3700 Sequence Detection System. Primers were designed and cDNA was reverse-transcribed as described above. Genomic DNA was obtained from DNA Resources at The Jackson Laboratory and used to amplify regions proximal to the coding region.

General statistical analyses

Plasma lipoprotein cholesterol concentration data are presented as "scattergram" plots. All other data are presented as mean ± SEM. Data were analyzed using Graphpad Prism (Windows v3.00, GraphPad Software, San Diego, CA). The lipoprotein cholesterol concentrations were analyzed using one-way ANOVA with Tukey's multiple comparison post-test. This statistical analysis was also used to confirm the allele effects at the peak QTL markers identified in the genome-wide scan for HDL, total cholesterol levels, and non-HDL cholesterol levels. $P < 0.05$ was considered significant. Phenotypes were associated using Pearson's correlation. Real-time PCR data were analyzed using Student's *t*-test.

RESULTS

Plasma lipoprotein cholesterol concentrations

To determine HDL, total cholesterol concentrations, and non-HDL cholesterol concentrations, male animals from the parental strains and the reciprocal F_1 progeny, (CAST × D2)F_1 and (D2 × CAST)F_1 lineages, were fed the lithogenic/atherogenic diet for 8 weeks (n = 10 per group). The results of the lipoprotein cholesterol determinations are presented in **Fig. 2** and **Table 2**. Compared with D2, CAST displayed significantly decreased HDL (Fig. 2A, Table 2), but significantly increased total cholesterol (Fig. 2B, Table 2) and non-HDL cholesterol (Fig. 2C, Table 2) levels. Because no difference was observed between male reciprocal F_1 progeny, the F_1 mice were grouped prior to comparison with the parental strains. The fact that reciprocal F_1 progeny displayed similar values indicated that these traits were not inherited by maternal or imprinted genetic factors in this cross. Therefore, autosomal chromosomal regions carrying genes determining these factors could be detected by QTL analysis with-

TABLE 1. Gene-specific oligonucleotide primers employed for real-time PCR

Gene Symbol Official (Common)	Chr[a] (cM)	Primer Sequences (5′–3′) Forward	Exon	Reverse	Exon	Amplicon	ENSEMBL Accession Identification
						bp	
Lrp2 (Megalin, Gp330)	2 (40.0)	tgtaccagaaaatgtggaaaacc	2	gtgtcttctgtggcagtgtagc	5	288	ENSMUST00000028462
Nr1h3 (Lxra)	2 (40.4)	agtgactgtttcaccgtgtcc	10	tatttggttgggtcaacaagg	10	231	ENSMUST00000002177
Abca1	4 (23.1)	accagaacatgggctactgc	44	ggagagctttcgtttgttgc	45	209	ENSMUST00000030010
A2m (Mam)	6 (62.0)	gggtacctgtccatttttactacg	10	taactctggcttggagaaaagact	11	200	ENSMUSG00000030359
Apobec1	6 (54.5)	tggaggaatttcgtcaactacc	7	catggcagtcactctttagtgg	8	326	ENSMUST00000043216
Lrp6	6 (63.9)	cagatgagaagaactgtgaagtgc	18-19	aatggtgacaattactccaataacg	20	203	ENSMUST00000032322
Pparg[b]	6 (52.7)	tccattcacaagagctgacc	2	ccggcagttaagatcacacc	4	301	ENSMUST00000000450
Ldlr	9 (5.0)	acatggtatgaggttcctgtcc	16	tctggagagagtgtcttttctgc	17	307	NM_010700.1[c]

cM, centimorgans. Primers were designed using the sequences indicated in the table. PCR products were subjected to gel (2.5%) electrophoresis with ethidium bromide staining or dissociation analysis using the real-time PCR machine to ensure specific amplification of a single product. The amplicon was directly sequenced and the sequence used to interrogate the public mouse genome (BLAST analysis in ENSEMBL) to ensure the identity of the amplicon.

[a] Candidate chromosome and position (cM).

[b] Oligonucleotide primers were designed to amplify both *Pparg1* and *Pparg2* mRNA transcripts.

[c] NCBI accession.

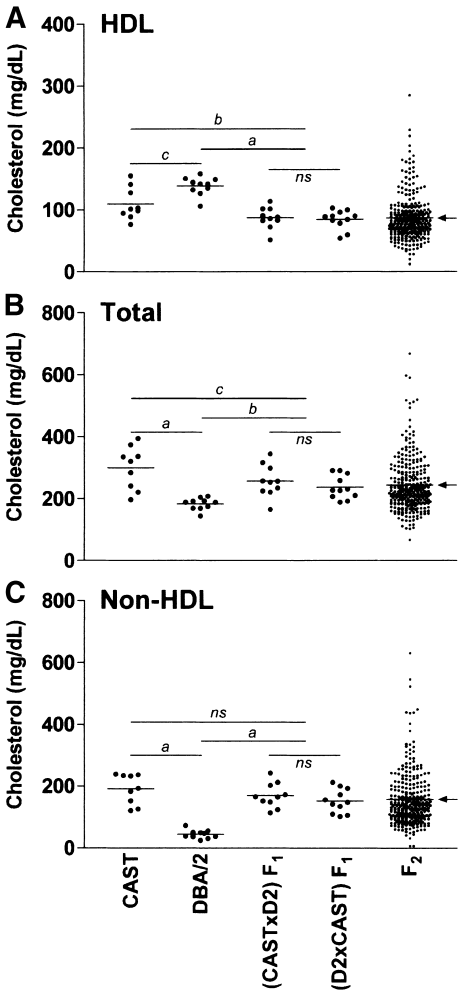

Fig. 2. Plasma lipoprotein cholesterol concentrations in male parental F_1 and F_2 populations. HDL (A) and total cholesterol (B) were determined using automated enzymatic assays. Non-HDL (C) was calculated as the difference between total and HDL cholesterol concentrations. Parental and F_1 mice were fed the lithogenic diet for 8 weeks, whereas F_2 mice were fed the diet for 10 weeks prior to cholesterol determinations. Reciprocal F_1 groups did not differ for any levels of HDL, total, or non-HDL cholesterol, and thus were grouped to compare with CAST/Ei (CAST) and DBA/2J (D2). Because it is the distribution and not the mean that is most important for detecting QTL among the F_2 population, we did not test for significant differences between this group and the parental strains or F_1 group. The mean values are indicated by bars and also by an arrow for the F_2 population. ^{a} $P < 0.001$; ^{b} $P < 0.01$; ^{c} $P < 0.05$; ^{ns} not significant. The lipoprotein cholesterol data were analyzed using one-way ANOVA with Tukey's multiple comparison post-test.

out the need to consider lineage-specific QTL effects. Surprisingly, the F_1 (and F_2) animals exhibited HDL cholesterol levels lower than both CAST and D2 (Fig. 2A, Table 2), indicating either that both strains contributed alleles leading to lower HDL cholesterol levels or that some alleles for higher HDL cholesterol levels may be inherited in a recessive fashion and therefore be obscured in the heterozygous state. The F_1 mice displayed total cholesterol levels intermediate between and significantly different from the parental strains (Fig. 2B, Table 2). Non-HDL cholesterol concentrations of the F_1 mice were comparable to strain CAST but significantly higher than strain D2 (Fig. 2C, Table 2); thus, high non-HDL cholesterol levels were inherited in a dominant fashion. Non-HDL and total cholesterol levels were correlated strongly (Pearson correlation coefficient 0.915, $P < 0.0001$), likely reflecting the fact that the total cholesterol is predominantly comprised of non-HDL cholesterol. Non-HDL cholesterol was negatively correlated with HDL cholesterol (coefficient −0.236, $P < 0.0001$), but HDL was not correlated with total cholesterol.

TABLE 2. Plasma lipoprotein cholesterol concentrations in male parental, F_1, and F_2 populations

Mice Population	No.	Lipoprotein Cholesterol					
		HDL		Total		Non-HDL	
		Mean	SEM	Mean	SEM	Mean	SEM
				mg/dl			
CAST	9	109.6	8.6^{a,b}	300.4	23.0^{d,e}	190.9	16.1^{g}
DBA/2	10	138.5	4.7^{a,c}	183.1	6.1^{d,f}	44.7	4.4^{g,h}
(CAST × D2)F_1	10	86.9	5.4	257.1	16.4	170.2	12.6
(D2 × CAST)F_1	11	84.1	4.7	236.8	11.5	152.6	11.7
Combined F_1	21	85.4	3.5^{b,c}	246.5	9.9^{e,f}	161.0	8.6^{h}
F_2	277	86.4	2.2	244.1	5.3	158.5	5.3

CAST, CAST/Ei; D2, DBA/2J; QTL, quantitative trait locus/loci. Parental and F_1 mice were fed the lithogenic diet for 8 weeks, whereas F_2 mice were fed the diet for 10 weeks prior to cholesterol determinations. Data were generated and analyzed as described in Fig. 2 and are presented as mean and SEM. Reciprocal F_1 groups did not differ for any of the lipoprotein cholesterol levels and thus were grouped to compare with CAST and D2. Because it is the distribution and not the mean that is most important for detecting QTL among the F_2 population, we did not test for significant differences between this group and the parental strains or F_1 group. Common superscript characters indicate pairs of significantly different groups.

^{a} $P < 0.05$.
^{b} $P < 0.01$.
^{c} $P < 0.001$.
^{d} $P < 0.001$.
^{e} $P < 0.05$.
^{f} $P < 0.01$.
^{g} $P < 0.001$.
^{h} $P < 0.001$.

To improve the phenotyping related to gallstone susceptibility, the feeding regimen for the F_2 population was prolonged from 8 weeks to 10 weeks (24). However, the distributions of the three cholesterol measurements in the F_2 animals did not appear unduly affected by the extended feeding period and were consistent with the data observed in the parental and F_1 mice (Fig. 2, Table 2). The decreased mean of the F_2 HDL cholesterol, compared with that of the F_1 group, may reflect the longer duration of feeding, since cholic acid is known to decrease HDL cholesterol levels (32, 33), apparently by down-regulating apoA-I transcription via a putative bile acid response element (34). Furthermore, because it is the distribution and not the mean among the F_2 population that is most important for detecting genetic linkage to a phenotype, we did not test for significant differences between this group and either the parental strains or F_1 group.

QTL analyses

We genotyped and performed QTL analyses on the entire group of F_2 mice (n = 278), initially employing 96

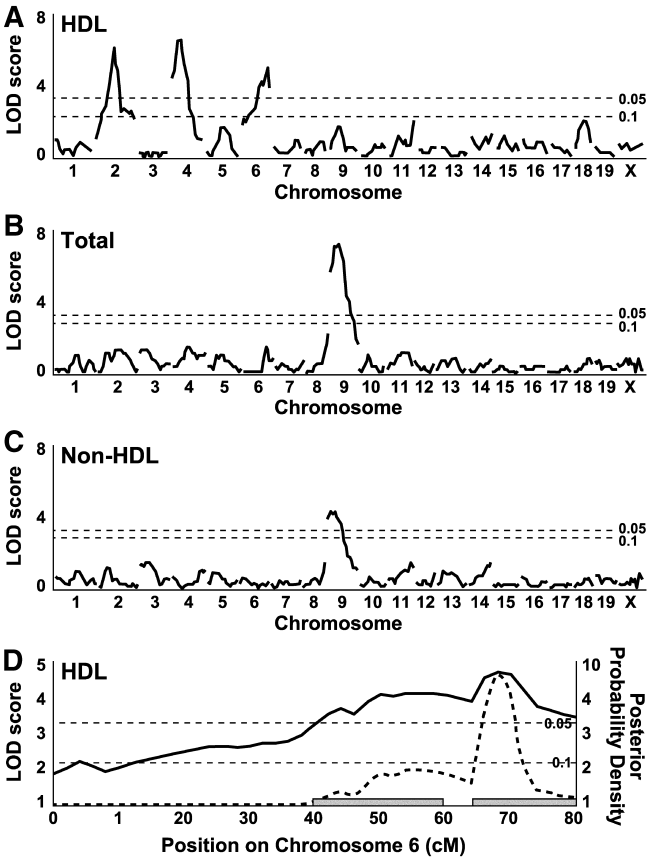

Fig. 3. Genome-wide QTL analyses for loci determining plasma lipoprotein cholesterol levels in the F_2 population derived from strains CAST and D2. Chromosomes 1 through X are represented numerically on the ordinate. The relative width of the space allotted for each chromosome reflects the relative number of SSLP markers of each chromosome. The abscissa represents the logarithm of the odds ratio (LOD) score, the traditional metric of genetic linkage. The significant ($P < 0.05$) and suggestive ($P < 0.10$) levels of linkage were determined by permutation testing (31). HDL cholesterol levels are presented in A; total cholesterol, B; non-HDL cholesterol, C. D: Represents the genome-wide scan for HDL cholesterol for chromosome 6 only (solid line). The posterior probability density (broken line) is a likelihood statistic that gives rise to the 95% confidence intervals that are indicated by the gray bars (29).

SSLP markers distributed across the genome for a preliminary QTL analysis. To refine the QTL intervals, we then increased the total number of SSLP markers to 109 [final interval range 1–27 centimorgans (cM)] by adding markers to selected QTL regions, particularly chromosomes 2 and 6. The genome-wide scans for single QTL are presented in **Fig. 3**. Significant QTL for HDL cholesterol were detected on three different chromosomes, chromosomes 2, 4, and 6 (Fig. 3A, D). One QTL was detected for total cholesterol (Fig. 3B) and one for non-HDL cholesterol (Fig. 3C); these were both linked to *D9Mit58*. Given the strong correlation between these two phenotypes, the data suggest the presence of a single locus. In total, the four QTL for HDL cholesterol accounted for 28.4% of the variance in the F_2 population, whereas the QTL for total cholesterol accounted for 11.2% of the F_2 variance (**Table 3**). Details of the QTL detected, including the LOD score (the traditional metric of genetic linkage), QTL peak, 95% confidence interval, variance, allele conferring, increased concentration, and candidate genes, are presented in Table 3 (the genetic positions of candidate genes are depicted in Fig. 1).

The QTL on chromosome 6 for HDL cholesterol (Fig. 3D) was fitted with models comprising one QTL, two QTL, or three QTL, and a maximum LOD score calculated for each. Permutation testing was used to determine significance thresholds. Increases of 2.0, 1.6, and 1.4 or greater in the LOD score were the thresholds used to declare multiple QTL at the 95%, 90%, and 80% confidence levels, respectively. We observed an increase of 2.6 LOD (3.2 vs. 5.8) for the one-QTL versus the two-QTL model, but an increase of only 0.5 LOD for the three-QTL model. Therefore, we conclude that two QTL on distal chromosome 6 contribute to HDL cholesterol concentrations (Fig. 3D, Table 3).

At each QTL, we determined the allelic contribution to the given phenotype. A recessive D2 allele at the QTL linked to *D2Mit94* was associated with higher HDL cholesterol (**Fig. 4A**). At the QTL for HDL linked to *D4Mit110*, a dominant or codominant CAST allele increased HDL cholesterol (Fig. 4B). Detecting a QTL inherited from the parental strain with lower HDL concentrations, CAST, that increased HDL cholesterol compared with the D2 allele at this locus is not surprising, since this is a phenomenon encountered frequently in QTL crosses (35). It indicates that for this complex trait, both parental strains carry alleles that influence HDL cholesterol levels in both directions. At both QTL linked to *D6Mit36* (Fig. 4C) and *D6Mit14* (Fig. 4D), codominant D2 alleles contributed to higher HDL cholesterol levels. A CAST allele was associated with higher total and non-HDL cholesterol levels at the QTL linked to *D9Mit58* (Fig. 4E). At this locus, the heterozygous animals displayed an intermediate phenotype, although they resembled the D2 parental strain more than CAST. Because high levels of non-HDL cholesterol were dominant in the F_1 (Fig. 2C, Table 2) but the QTL at *D9Mit58* was inherited recessively, other alleles that were not detected in this analysis are likely to contribute to the phenotype.

The second stage of the QTL analysis was used to detect gene-gene interactions (epistasis). Using our criteria for significance (30), no interacting QTL were detected in this intercross. Therefore, only single QTL are presented. We named the significant loci for HDL cholesterol HDL QTL (*Hdlq*) followed by a number. The significant locus for total cholesterol was named *Chol* followed by a number. Therefore, the novel QTL for HDL cholesterol on chromosome 4 was named *Hdlq10*. Similarly the novel QTL on chromosome 6 were named *Hdlq11* (proximal) and *Hdlq12* (distal). The novel QTL for total cholesterol (and non-HDL) was named *Chol6*. The QTL for HDL cholesterol on chromosome 2 confirmed a locus identified earlier using a breeding cross employing different inbred mouse strains [previously named *Hdl1* (36)]. *Hdlq10* colocalized with a locus identified recently for the same trait using a mutagenesis approach; this locus was named *Lch* (37) (Table 3). A QTL found in a human study (38) was orthologous with *Hdlq10*, and both mouse and human regions harbored the *Abca1/ABCA1* lo-

TABLE 3. QTL for plasma lipoprotein cholesterol concentrations identified in the CAST × D2 intercross

Locus (cM)	QTL Name	Phenotype	Chr[a]	LOD[b]	QTL Peak	Variance	High Allele	Overlapping QTL[d]		Candidate Genes (cM)
								Name	Reference	
					cM (CI[c])	%				
D2Mit94 (48.1)	*Hdl1*	HDL	2	5.4	48 (44–56)	8.5	D2	*Hdl1*	(36)	*Lrp2* (40.0), *Nr1h3* (40.4)
D4Mit110 (21.9)	*Hdlq10*	HDL	4	5.9	20 (10–30)	9.3	CAST	*Lch*[e]	(33, 37)	*Abca1* (23.1)
D6Mit36 (46.0)	*Hdlq11*	HDL	6	4.2	48 (40–60)	5.3	D2			*Apobec1* (54.5), *Pparg* (52.7)
D6Mit14 (71.2)	*Hdlq12*	HDL	6	4.9	68 (64-80)	5.3	D2			*A2m* (62.0), *Lrp6* (63.9)
D9Mit58 (5.0)	*Chol6*[f]	Total	9	7.2	8 (5–27)	11.2	CAST	—	(36)[g]	*Ldlr* (5.0)
D9Mit58 (5.0)	*Chol6*[f]	Non-HDL	9	4.6	6 (4–25)	7.3	CAST			*Ldlr* (5.0)

LOD, logarithm of the odds ratio.
[a] Chromosome.
[b] Suggestive QTL LOD ⩾ 2.2, significant QTL LOD ⩾ 3.3.
[c] 95% Confidence interval.
[d] Overlapping QTL identified in previous studies.
[e] Point mutation from a mutagenesis experiment, not a QTL, which colocalizes with *Hdlq10* for the same phenotype (HDL).
[f] Because the correlation of total with non-HDL cholesterol levels was so strong (Pearson's coefficient 0.915, $P < 0.0001$) and because the allele effects (Fig. 4E) and the genetic position of these loci were virtually indistinguishable, it is probable that these QTL are identical.
[g] QTL found on chow, peak 17 cM.

cus. Furthermore, a QTL for LDL was detected on human chromosome 19 (39), a portion of which is orthologous with mouse chromosome 9, and contains *LDLR*.

Candidate gene expression analyses

To identify genes that colocalized with the QTL and that were involved in lipid metabolism (candidate genes), we scrutinized the public genome databases (Table 3, Fig. 1). Because overall HDL levels are determined by the liver (8), the candidate genes were tested for differential hepatic mRNA expression between the parental strains, CAST and D2, and selected mice from the F_2 population possessing either homozygous CAST or homozygous D2 alleles in the regions of interest (**Fig. 5**).

We tested two candidate genes for *Hdl1* (chromosome 2): *Lrp2* (*Megalin, Gp330*; 40.0 cM) and *Nr1h3* (*Lxra*; 40.4 cM). No differential mRNA expression was detected for *Lrp2* (Fig. 5A). CAST displayed a small but significant increase in *Nr1h3* mRNA expression amounting to a 2-fold increase (Fig. 5A). For *Hdlq10* (chromosome 4), we identified *Abca1* as a physiologically relevant and highly attractive candidate gene. CAST displayed higher expression of *Abca1*, amounting to a 4-fold difference between strains (Fig. 5A). *Hdlq11* (chromosome 6) encompassed candidate genes including *Apobec1* and *Pparg*. *Apobec1* expression was 2.8-fold higher in CAST compared with D2 mice (Fig. 5A). Conversely, D2 exhibited a 4.7-fold higher mRNA expression of *Pparg* (Fig. 5A). Candidate genes for *Hdlq12* (chromosome 6) included *A2m* and *Lrp6*. D2 mice exhibited significantly higher mRNA expression levels of these two genes compared with CAST, amounting to 6.9- and 2.5-fold, respectively (Fig. 5A). Finally, *Ldlr* was a particularly strong candidate gene for *Chol6* (chromosome 9). D2 displayed a markedly increased expression of *Ldlr* compared with CAST (Fig. 5A), amounting to a 18-fold increase over strain CAST. Therefore, all of the candidate genes tested, excluding *Lrp2*, displayed differential expression and warranted further investigation with respect to the mRNA expression characteristics.

Intercross progeny inherit unique combinations of alleles derived from both parental strains. Therefore, when differential expression of a candidate gene is demonstrated for animals that are homozygous for one parental strain versus the other only in the region harboring the candidate gene, it provides strong support for *cis*-acting elements rather than *trans*-acting elements remote from the gene of interest. Hence, we proceeded to investigate further the QTL for lipoprotein cholesterol in the F_2 population. We selected individual samples that were either homozygous CAST or homozygous D2 over the loci on chromosomes 2, 4, 6, and 9. We determined the mRNA expression levels for *Lrp2*, *Nr1h3*, *Abca1*, *A2m*, *Apobec1*, *Lrp6*, *Pparg*, and *Ldlr*. *Nr1h3* expression was significantly increased, albeit modestly, in F_2 animals possessing homozygous CAST alleles compared with D2 alleles (Fig. 5B). We confirmed that *Lrp2* was not differentially expressed between animals possessing homozygous CAST compared with D2 alleles (Fig. 5B). Likewise, it was established that *A2m*, *Apobec1*, and *Lrp6* did not display differential expression in the F_2 population (Fig. 5B). Conversely, *Pparg* demonstrated marked differential expression in the F_2 animals amounting to a 12.5-fold increase in strain D2 (Fig. 5B). *Abca1* was expressed 2.4-fold higher in F_2 mice bearing CAST alleles compared with those with D2 alleles, whereas the converse was true for *Ldlr*, which was expressed 6.1-fold higher by mice with D2 alleles versus CAST alleles (Fig. 5B). In summary, we find that three candidate genes displayed differential expression both between the parental strains, CAST and D2, and between animals possessing either homozygous CAST or homozygous D2 alleles derived from the F_2 population. These data indicate likely *cis*-acting elements that determine *Hdlq10* (*Abca1*), *Hdlq11* (*Pparg*), and *Chol6* (*Ldlr*).

Candidate gene sequence analysis

Because nuclear transcription factors, i.e., *Nr1h3* and *Pparg*, hold great potential to influence the transcription of

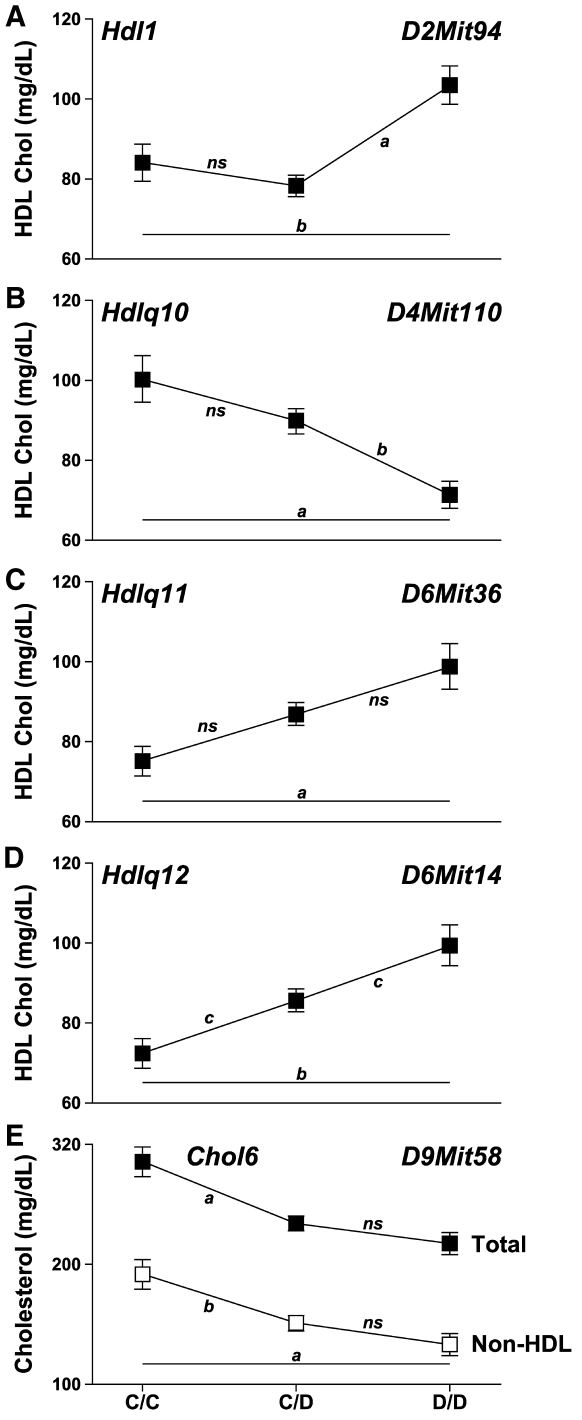

Fig. 4. Allelic contributions to the QTL detected on chromosomes 2, 4, and 6 for HDL, and on chromosome 9 for total and non-HDL cholesterol concentrations. Homozygous CAST alleles are represented by C/C, homozygous D2 alleles by D/D, and heterozygous alleles by C/D. A recessive D2 allele at *Hdl1*, linked to *D2Mit94*, was associated with higher HDL cholesterol (A). A dominant or codominant CAST allele determined increased HDL cholesterol levels at *Hdlq10* that were linked to *D4Mit110* (B). At both *Hdlq11* and *Hdlq12*, linked to *D6Mit36* and *D6Mit14*, respectively, codominant D2 alleles contributed to higher HDL cholesterol levels (C, D). *Chol6*, linked to *D9Mit58*, was detected for total (filled) and non-HDL cholesterol (open) concentration, and is likely the same locus (E). A recessive (or codominant) CAST allele was associated with higher total and non-HDL cholesterol levels at *Chol6*. Data represent mean ± SEM. $^{a}P < 0.001$; $^{b}P < 0.01$; $^{c}P < 0.05$. The line positioned above the ordinate indicates the result of one-way ANOVA.

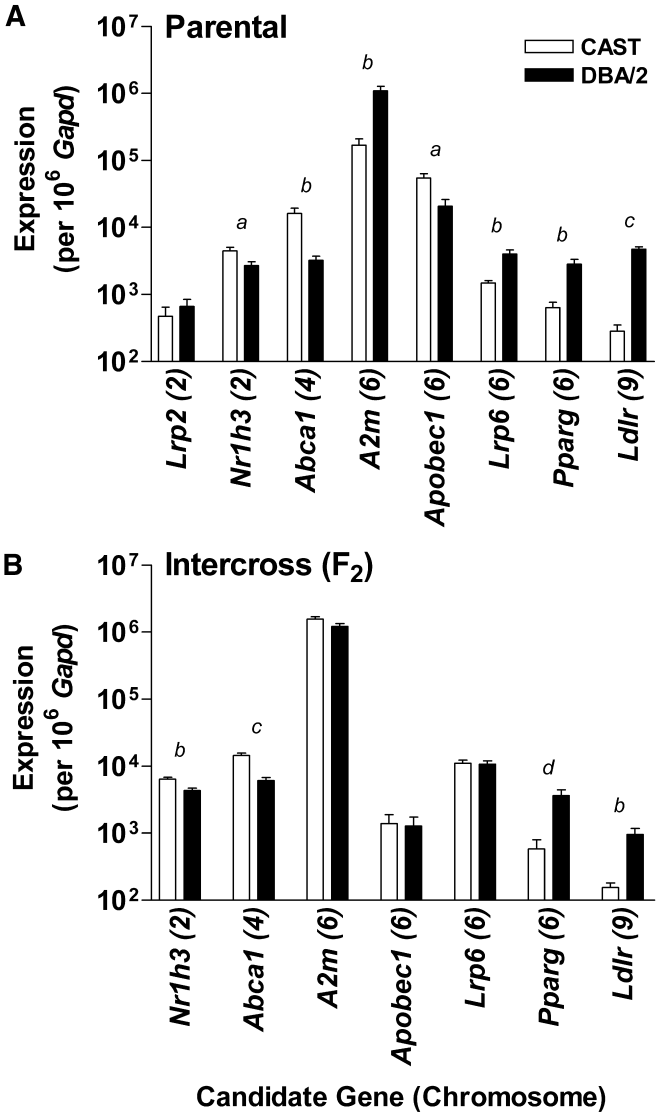

Fig. 5. Hepatic mRNA expression analysis of positional candidate genes identified for the QTL on chromosomes 2, 4, 6, and 9. The candidate gene is indicated on the ordinate with the chromosome number following in parentheses. Parental animals (CAST, open; D2, filled; A) were fed the lithogenic diet for 4 weeks prior to collection of liver tissue. Liver tissue from F_2 animals (B) homozygous for CAST (open) or D2 (filled) alleles over the *Hdl1*, *Hdlq10*, *Hdlq11/ Hdlq12*, and *Chol6* QTL were collected after 10 weeks' feeding. Samples were prepared as described. Gene-specific oligonucleotide primers were employed to analyze candidate genes using real-time PCR. Data are reported as the number of target molecules per 10^6 *Gapd* molecules (mean ± SEM; mean of three separate determinations, except F_2 *Abca1* and *Ldlr* mean of 2 separate determinations; n = 5 animals per parental group; n = 10–15 animals per F_2 group). The two groups of animals for each candidate gene were compared using Student's *t*-test. $^{a}P < 0.05$; $^{b}P < 0.005$; $^{c}P < 0.0001$; $^{d}P < 0.001$.

a wide array of lipoprotein metabolic proteins, we sequenced the coding region of *Pparg* and both the coding region and ~750 nucleotides proximal to the transcription start site of *Nr1h3* (GenBank accession AY195870, CAST; AY195871, D2). Six single-nucleotide polymorphisms (SNPs) were detected between CAST and D2 in the coding region of *Nr1h3*, but all were silent mutations bearing no ef-

TABLE 4. Summary of nucleotide sequence variations in the coding region of *Pparg* (GenBank accession AY208183, CAST/Ei; AY208184, DBA/2J) and both the coding and promoter regions of *Nr1h3* (GenBank accession AY195870, CAST; AY195871, D2) detected between strains CAST and D2

Candidate	Region	Variant	Position	Effect on Coding
Nr1h3	Promoter	G-743A		
	Promoter	T-742G		
	Promoter	A Deletion	−731	
	Promoter	C-720T		
	Promoter	C-682T		
	Promoter	T-611C		
	Promoter	G-610A		
	Promoter	$(TTTG)_4$ Insertion	−541 to −552	
	Promoter	A-528C		
	Promoter	A-469T		
	Promoter	C-453T		
	Promoter	T-376C		
	Promoter	G-357C		
	Promoter	G-354C		
	Promoter	G-345A		
	Promoter	GTGGGGG Deletion	−319 to −325	
	Promoter	C-26A		
	Promoter	T-16A		
	Exon1, 5′ UTR	C126G		
	Exon 4	T558C		Silent
	Exon 5	T870C[a]		Silent
	Exon 5	A873G		Silent
	Exon 7	T1068C[a]		Silent
	Exon 10	G1385C[b]		R399P
	Exon 10	A1398T		Silent
	Exon 10	T1428G		Silent
Pparg	Exon 3	C537T		Silent
	Exon 5	T1053C		Silent
	Exon 6	T1395C		Silent
	Exon 6, 3′ UTR	A Deletion	1,619	

All positions are given relative to the transcription start site of the aligned sequences. All variations are given relative to strain D2.

[a] 129/SvJ possesses C at positions 870 and 1,068 (GenBank accession NM_013839).

[b] CAST and D2 both possessed C at position 1,385 whereas 129/SvJ was reported to possess G.

fect on the amino acid sequence (**Table 4**). Fifteen SNPs were identified upstream of the transcription start site. One SNP was detected at position +126 of the 5′ untranslated region of Exon 1. In addition, based on the aligned sequences, CAST displayed a 7-nucleotide deletion relative to D2 (GTGGGGG, position −319 to −325 relative to transcription start site), whereas D2 exhibited a 12-nucleotide deletion comprising three repeats of a TTTG motif (position −541 to −552). CAST also displayed a single adenosine deletion at position −731. We identified no sequence differences leading to altered amino acid residues in the *Pparg* transcript (Table 4; GenBank accession AY208183, CAST; AY208184, D2). Therefore, functional differences of NR1H3 and PPARγ were excluded because the amino acid sequence was conserved. However, *Nr1h3* expression differences may be accounted for by the polymorphisms proximal to the transcription start site and in the 5′ untranslated region. Other investigators reported differences between CAST and C57BL/6 mice in the promoter region of *Pparg* (36). It remains to be determined if such differences or other unique variations exist between CAST and D2.

DISCUSSION

Studies indicate that complex genetic bases determine individual HDL cholesterol concentrations in response to environmental factors (18). Knowledge of the primary genetic determinants of plasma lipoprotein levels will enhance our understanding of lipoprotein metabolism and likely provide novel molecular targets for new or enhanced therapy for diseases such as atherosclerosis (3). Advantages of this phenotype-driven method are *i*) detection of rate-limiting genetic defects; *ii*) discrimination of rate-limiting defects from secondary (downstream) effects; and *iii*) identification of novel genes or identification of known genes with novel functions. Once murine genes have been identified, researchers can predict the position and function of the orthologous human genes. To date, including the present study, more than 20 loci have been identified influencing HDL cholesterol levels alone (18).

We fed a high-cholesterol cholic acid diet to our experimental animals. Cholic acid is known to decrease HDL levels in some strains of mice (32–34), primarily via a putative bile acid response element that mediates transcriptional repression of apoA-I (34). However, despite this observation, most QTL for HDL phenotypes tend to colocalize irrespective of the experimental diet (18). Therefore, we believe that the loci described in the present study make valid contributions to our understanding of the genetic control of lipoprotein metabolism.

Using an intercross between the wild-derived inbred strain CAST and the inbred strain D2, we have detected four QTL for HDL cholesterol concentration (chromosomes 2, 4, and two on 6), and one QTL that was detected for both total and non-HDL cholesterol levels (chromosome 9) (Fig. 3). Lipoprotein phenotypes constitute a physiological continuum or distribution. Thus far, animal models describe the genetic extremes of null expression (knockout) and overexpression (transgenic). The HDL cholesterol QTL linked to *D4Mit110* (peak 21.9 cM; *Hdlq10*) and the total and non-HDL cholesterol QTL linked to *D9Mit58* (peak 5.0 cM; *Chol6*) comprise compelling genetic evidence for the existence of alleles that contribute to that distribution but fall between those two extremes. The candidate gene for *Hdlq10* is *Abca1* (23.1 cM), encoding the ATP binding cassette cholesterol-phospholipid transporter ABCA1, and for *Chol6* is *Ldlr* (5.0 cM), encoding LDL receptor (Ldlr), each of which profoundly influences lipoprotein homeostasis in both humans (10, 11, 16) and mice (40–47). We confirmed with an independent cross a QTL for HDL cholesterol reported previously on chromosome 2 (*Hdl1*). In addition, this locus colocalized with another QTL for obesity (*Mob6*) that was also associated with HDL (36, 48), but may not be an HDL locus because many obesity mutations in mice affect HDL concentrations (49). Furthermore, we report two novel QTL for HDL in close proximity on distal chromosome 6 (*Hdlq11* and *Hdlq12*). Preliminary evaluations of candidate genes for the novel QTL are reported. In addition, we assessed candidate genes according to literature describing their effects on HDL, total cholesterol, or non-

HDL cholesterol levels with regard to decreased (knockout mice) and increased (transgenic mice) gene expression. These results are summarized in **Table 5**.

Nonfunctional Ldlr was demonstrated to be the monogenic cause of human familial hypercholesterolemia (16). *Ldlr* knockout mice (40) also exhibited massive increases in non-HDL cholesterol, whereas *Ldlr* transgenic mice (41, 42) virtually eliminated LDL from the plasma due to increased hepatic uptake. Because total cholesterol and non-HDL cholesterol levels correlated with such strength and because the allele effects (Fig. 4E) and genetic position of the loci (Table 3) were virtually indistinguishable, it is probable that these loci identified a single QTL. One QTL for plasma total cholesterol (*D9Mit2*) was found to overlap using a B6 × CAST intercross (36). CAST conferred the allele linked to increased plasma cholesterol in that study (36), in agreement with our findings (Fig. 4E). A QTL for LDL cholesterol was detected within 20 cM of *Ldlr* on human chromosome 19 (39), portions of which are orthologous with mouse chromosome 9 and contain *Ldlr*. Consistent with the role of Ldlr and their increased total and non-HDL cholesterol levels, CAST mice expressed *Ldlr* at a markedly decreased level relative to D2 (Fig. 5A). A previous investigation demonstrated a prominent increase in VLDL, IDL, and LDL cholesterol levels of CAST mice fed a similar cholesterol-cholate diet (36). The observed increase in cholesterol was due to VLDL predominantly (36). Because Ldlr does not mediate VLDL uptake, that finding likely explains our observation that *Chol6* accounted for a maximum of only 11% of the variance in plasma total cholesterol (Table 3), further substantiating the implication that other loci, not detected in this cross, contribute to non-HDL cholesterol concentrations. Taking all results together (Table 5), the data clearly support the candidacy of *Ldlr* as a primary genetic determinant of murine total and non-HDL cholesterol concentrations. We speculate that alleles may exist that contribute to variations of Ldlr activity in the human population.

In a manner similar to the genetics of Ldlr and familial hypercholesterolemia patients, nonfunctional ABCA1 in human Tangier's disease patients results in extremely low HDL cholesterol levels and premature atherosclerosis (10, 11). *Abca1* knockout mice (43–45) also display dramatically decreased HDL cholesterol, whereas *Abca1* transgenic mice (46, 47) display increased HDL cholesterol levels. Their effects on HDL cholesterol were consistent with *Abca1* being the polymorphic gene underlying *Hdlq10* (Table 5). A similar QTL for HDL cholesterol was detected using an intercross between strains C57BL/6J (B6) and C3H/HeJ (peak 21.9 cM) (33), and a polymorphism causing decreased HDL levels was identified in a mutagenesis experiment involving strains Balb/c and C3H/HeH (*Lch*, peak 26.7 cM) (37). Linkage studies performed in an Hispanic population indicate that HDL cholesterol levels are influenced by a QTL harboring the *ABCA1* locus (38), and polymorphisms in the promoter of

TABLE 5. Effect of allele status and genetic manipulation on plasma cholesterol concentrations in parental, intercross, knockout, and transgenic murine models

QTL Name	Candidate Gene	Chr[a]	Allele Effect[b]			Effect on HDL cholesterol[c]				Candidacy[d]	Notes
				Expression							
			QTL	P	F_2	KO	Ref[e]	TG	Ref[e]		
Hdl1	*Lrp2*	2	D2	↔	↔	?	(53)	—		—	KO neonatal lethal; predominantly expressed in kidney, small intestine, yolk sac, and placenta (52); low hepatic expression.
Hdl1	*Nr1h3*	2	D2	CAST	CAST	↓	(55, 56)	—		No	Mild decrease of HDL in KO results duplicated by two separate laboratories.
Hdlq10	*Abca1*	4	CAST	CAST	CAST	↓	(43–45)	↑	(47)	Yes	
Hdlq11	*Apobec1*	6	D2	CAST	↔	↔, ↓	(62, 64–66, 78)	↑, ↔, ↓	(67, 69, 70)	No	KO animals with decreased levels were generated in 129/J embryonic stem cells and maintained in a mixed C57BL/6, DBA/2 background (65). TG generally indicates no change; one report displays mild decrease; TG rabbit (n=1) displayed increased HDL (68).
Hdlq11	*Pparg*	6	D2	D2	D2	?	(58)	—		Yes	KO embryonic lethal.
Hdlq12	*A2m*	6	D2	D2	↔	?	(74)	—		No	A2m inhibits LCAT activity and mediates LCAT hepatic uptake and therefore may influence HDL maturation (73).
Hdlq12	*Lrp6*	6	D2	D2	↔	?	(75)	—		No	KO embryonic lethal.
Chol6	*Ldlr*	9	CAST	D2	D2	↑	(41, 42)	↓	(40)	Yes	

F_2, intercross; KO, knockout; P, parental; TG, transgenic. Literature searches were performed to identify publications describing genetic manipulation of candidate genes. The data presented in those publications were interpreted to be consistent or inconsistent with gene candidacy with respect to the QTL location, allelic contribution, and mRNA expression data generated in this study.

[a] Chromosome.

[b] Allele determining high phenotype and high expression.

[c] Non-HDL cholesterol for *Ldlr*, Chr 9.

[d] Overall consistency with observed allele effect and mRNA expression data leading to assessment of candidacy.

[e] Reference.

ABCA1 were associated with HDL cholesterol levels in a second human population (50). We showed that CAST contributed the allele associated with increased HDL cholesterol levels at this locus (Fig. 4B), and confirmed that the expression of *Abca1* was greater in that strain compared with D2, the strain contributing the allele for low HDL cholesterol (Fig. 5A). The evidence indicates that at least one polymorphism exists in the murine *Abca1* gene or its regulatory regions that affects HDL cholesterol concentrations. We postulate that *ABCA1* exists in polymorphic forms and contributes to the variability of the HDL phenotype in humans.

In addition to *Hdlq10* and *Chol6*, we identified one QTL for HDL cholesterol on chromosome 2 (*D2Mit94*, *Hdl1*). Positional candidate genes include *Lrp2* (*Megalin*, *Gp330*; 40.0 cM) and *Nr1h3* (*Lxra*; 40.4 cM), although both lie outside the 95% confidence interval. LRP2 was reported to interact with CUBN (*Cubn*, 9.0 cM) to mediate HDL uptake in vitro, but neither transcript was expressed in the liver (51). To date, little evidence is available indicating that hepatic expression is substantial (52). Although we were able to amplify the transcript (Fig. 5A) from liver tissue, we failed to detect any differential expression of *Lrp2* between the two parental strains or in the F_2 population (Fig. 5A, B). Furthermore, we consider it unlikely that other tissues expressing LRP2 would remove enough HDL from the circulation to affect overall levels. *Lrp2* knockout mice (53) demonstrated embryonic lethality with predominant renal and very low hepatic expression (Table 5). No report was made regarding plasma lipoprotein status (53). It cannot be excluded that polymorphisms in the coding sequence led to analtered amino acid sequence and therefore altered function that affected HDL cholesterol levels. Given the tissue distribution data (52) and inferred low capacity to modulate HDL cholesterol levels, however, such a hypothesis is not considered a strong possibility.

The second candidate gene we identified for *Hdl1* was *Nr1h3* (*Lxra*, 40.4 cM) encoding the ligand-activated nuclear transcription factor NR1H3/LXRα. *Nr1h3* is an attractive candidate, especially because its target genes include *Abca1*, *Apoe*, *Lpl*, and *CETP* (in humans) encoding ABCA1, apoE, lipoprotein lipase, and cholesteryl ester transfer protein, respectively (54). We envisaged *Nr1h3* upregulation to increase HDL cholesterol accordingly. In our present study, both CAST mice and F_2 animals with CAST alleles across the locus exhibited greater hepatic expression of *Nr1h3* (Fig. 5) and decreased levels of HDL cholesterol (Fig. 2A and Table 2). However, D2 contributed the high allele for this QTL (Fig. 4A). We eliminated the possibility that a functional polymorphism (i.e., coding sequence variant causing amino acid change) was responsible for the QTL. The sequencing data may explain the differential mRNA expression, however, because a variety of polymorphisms were identified in the proximal noncoding region that likely harbors regulatory elements. Independently generated *Nr1h3* knockout mice displayed mild but consistent decreases in HDL cholesterol levels (55, 56). No report has yet appeared on a transgenic *Nr1h3* mouse. Therefore, both expression and sequence data are inconsistent with both the allele effect and the description of the murine knockout model (Table 5). The fine-mapping that indicates *Nr1h3* lies outside of the 95% confidence interval (Table 3) adds further validity to the conclusion that *Nr1h3* is not responsible for *Hdl1*.

Because *Pparg* is strongly expressed in the liver parenchymal cells (57) and encodes a nuclear transcription factor involved in lipid homeostasis, we deemed it an attractive candidate gene for the QTL on proximal chromosome 6 that controls HDL cholesterol. However, genetic modification of the *Pparg* gene did not yield the instructive findings that were anticipated. Knockout mice were generated but found to be embryonic lethal (58), and hence yielded no data with regard to phenotypes such as the model's lipoprotein profile and transgenic mice have not been produced. In other studies, synthetic PPARγ ligands were shown to decrease HDL cholesterol in female mice but not male mice with the B6-*Ldlr* knockout background (59). The authors of the *Pparg* knockout study suggested, with supporting pharmacological and genetic data, that PPARγ might be a transcriptional activator when a ligand is bound, but in the absence of a ligand may act as a sequence-specific transcriptional repressor (60). If we disregard the potential confounders of gender and genetic background, one plausible explanation is that, due to its greater *Pparg* expression, D2 may possess a greater propensity to ameliorate the reduction in HDL, given equal availability of an appropriate ligand in both strains. Such an interpretation would account for both the increased mRNA expression (Fig. 5) and the allele associated with increased HDL levels (Fig. 4C) attributed to strain D2. These data support a role for PPARγ in HDL metabolism but are far from conclusive. Furthermore, the available data render it apparent that PPARγ possesses myriad roles in lipid metabolism (61) apart from its putative effect upon HDL.

A second gene we evaluated for *Hdlq11* was *Apobec1*, because the protein it encodes is involved in lipoprotein assembly (62). In a previous study, *Pparg* and *Apobec1* were evaluated as candidate genes in a B6.CAST congenic that was constructed to investigate an atherosclerosis QTL (*Artles*, peak 61.0 cM) (63) that overlapped *Hdlq11* and *Hdlq12*. Whereas *Apobec1* displayed no differential expression between B6 and CAST, *Pparg* expression was determined by *cis*-acting elements, and CAST alleles determined decreased expression (63). These data are consistent with our findings between CAST and D2 (Fig. 5), and therefore *Apobec1* was considered a poor candidate in both studies. A six-nucleotide deletion was detected 456 nucleotides upstream from the CAST *Pparg2* translation start site, potentially explaining the difference in transcription (63). We confirmed the existence of such a deletion between strains CAST and D2 in addition to a number of SNPs (24). Two independent investigations (62, 64) reported that *Apobec1* knockout mice display no change in HDL cholesterol concentrations when on the chow diet (Table 5). A third study indicated that the knockout mice displayed decreased HDL cholesterol, but the mixed genetic background of

these mice may have influenced the data (65). One published report indicated that *Apobec1* knockout mice fed a high-fat diet do not display altered HDL cholesterol levels either (66). Results from studies of *Apobec1* transgenic mice are inconsistent. The first study indicated that total cholesterol did not change but apoE and apoA-I (both protein constituents of HDL) increased (67). A second study did not report the effect of transgene insertion in mice but reported that HDL increased in one transgenic rabbit (68). A third study of *Apobec1* on an Ldlr knockout background indicated no change in HDL cholesterol (69), whereas a fourth study using a mixed genetic background indicated a decrease in HDL cholesterol (70). On balance, it appears that *Apobec1* has little effect on HDL cholesterol levels, at least when mice are fed chow.

Recently, a transcriptional cascade was described in macrophages whereby PPARγ activation mediated *Nr1h3* transcription that, in turn, increased *Abca1* transcription (71). It is tempting to speculate that we observed such a pathway because HDL cholesterol QTL were detected in the region of each gene (chromosomes 2, 4, and 6; Fig. 3A, Table 3). However, there are a number of factors that argue against this possibility: *1*) macrophage-derived HDL cholesterol contributes very little to overall levels (8, 72), although we did not measure cell-type-specific expression and therefore cannot rule out the possibility that hepatocytic expression of *Pparg* drives this pathway in the liver; *2*) the allelic effect and mRNA expression were not consistent at each of the loci; *3*) we detected no epistasis; and *4*) the F_2 mice that were tested for expression of *Nr1h3* and *Pparg* were selected only for one of the two respective regions and otherwise possessed unique combinations of alleles making it unlikely that such a pathway was functional. We tested the final point empirically and found that F_2 mice selected for their genotype at the *Pparg* locus did not differentially express *Nr1h3* or *Abca1* (data not shown). We interpret the findings to indicate that we detected three independent loci that influence HDL cholesterol levels but are not involved in a transcriptional cascade, specifically, a cascade involving *Pparg*, *Nr1h3*, and *Abca1*. It should be noted, however, that we cannot exclude the possibility that increased hepatocytic expression of *Pparg* may drive *Abca1* expression and thus increased HDL levels, but that the effect was masked by the presence of an independent QTL at the *Abca1* locus.

For the QTL linked to HDL on distal chromosome 6, *Hdlq12*, we considered *A2m* (62.0 cM) a candidate gene. α_2-Macroglobulin was shown to interact with LCAT, inhibiting its activity and leading to its clearance from the circulation (73), thereby providing a potential mechanism to affect HDL maturation and concentration. Investigation of CAST and B6 mice revealed a functional LCAT deficiency in strain CAST that was not due to genetic differences in *Lcat*, thereby explaining the absence of a QTL in that region (36). We report that *A2m* expression was not likely dictated by *cis*-acting elements (Fig. 5B) and in this sense, *A2m* is not considered a strong candidate. However, we did not investigate the possibility that *A2m* exists as a functional isozyme due to altered amino acid sequences. *A2m* transgenic mice are not reported thus far, whereas knockout mice were generated but no report was made on plasma lipoprotein profiles (74). *Lrp6* (the second candidate gene for *Hdlq12*) knockout mice exhibited embryonic lethality, and the data indicate a role for LRP6 in development and signal transduction (75). Transgenic animals have not been described. Combined with the mRNA expression data (Table 5), *Lrp6* seems unlikely to be a candidate gene influencing lipoprotein cholesterol concentrations.

Previous studies using CAST × B6 intercrosses reported a QTL for multigenic obesity (*Mob6/D2Mit14*, 49.6 cM) that was also linked to HDL cholesterol (36, 48) and colocalized with the chromosome 2 QTL reported herein. *Mob6* was strongly linked to HDL levels after feeding a high-fat diet, and in further agreement with our data (Fig. 4A), CAST contributed the low HDL cholesterol allele (36, 48). The two QTL determining HDL cholesterol concentrations detected on distal chromosome 6 (*Hdlq11*, 48.0 cM and *Hdlq12*, 68.0 cM) overlapped QTL for atherosclerosis [*Athsq2*, 62.0 cM (76), *Artles* 61.0 cM (63)] and bone density [*Bdt3*, 67.0 cM (77)]. Potentially, the atherosclerosis loci may be associated with HDL, whereas *Bdt3* was pleitropic with a QTL for HDL cholesterol level (77). The *Artles* QTL also coincided with a QTL controlling insulin concentrations (63), perhaps alluding to the involvement of PPARγ. Using our CAST × D2 intercross, we observed colocalizing QTL for cholesterol gallstones and HDL cholesterol on chromosomes 2 and 6 (24). These findings are reminiscent of QTL for HDL that were coincident with loci for *Cyp7a1* mRNA levels (33). Taken together, these data suggest that alleles exist on both chromosomes 2 and 6 that affect a variety of lipid-related traits and are coupled via the common HDL phenotype.

In this study, we have described four QTL for HDL cholesterol levels that localized to chromosomes 2, 4, and 6 (two loci). We also described colocalizing QTL for total and non-HDL cholesterol levels on chromosome 9 that we believe are determined by the same locus (*Chol6*). We evaluated four candidate genes for *Hdlq11* and *Hdlq12*; *Apobec1*, *Lrp6*, and *A2m* seem unlikely candidates in light of our and others' genetic data (Table 5). Conclusions are difficult to make with our current knowledge of PPARγ activity, but *Pparg* remains an appealing candidate gene for *Hdlq11*. Compelling candidates for the distal QTL remain to be evaluated but may include genes such as *Olr1* (76) (mapped to distal chromosome 6 by orthology and ENSEMBL database) or perhaps *Slc21a1* (24), considering the suggested link between bile acid metabolism and lipoprotein metabolism. We provide evidence suggesting that neither the nuclear oxysterol receptor NR1H3 (LXRα) nor LRP2 are determinants of HDL cholesterol. Candidates for *Hdl1* remain to be determined. Finally, excellent candidate genes were identified and evaluated for the loci on chromosomes 4 (*Abca1*, *Hdlq10*) and 9 (*Ldlr*, *Chol6*). In combination with previously reported data, we conclude that *Abca1* and *Ldlr* are likely primary genetic determinants of HDL cholesterol and total/non-HDL cholesterol, respectively. Moreover, we predict that these genes are

present in the human population as a wide repertoire of polymorphic alleles that contribute to the continuum of plasma lipoprotein cholesterol phenotypes.

This study was supported in part by National Institutes of Health Grants DK-51568 (to B.P.); DK-36588, DK-52911, and DK-34854 (to M.C.C.); and CA-34196 (core grant to The Jackson Laboratory). M.A.L. was supported by the American Physiological Society and the American Liver Foundation. H.W. (WI 1905/1-1) was supported by the Deutsche Forschungsgemeinschaft. We are greatly indebted to Dr. Jason Stockwell, Jennifer Smith, and Susan Sheehan (The Jackson Laboratory) for consultation on general statistical methods and assistance with graphics and sequencing of PCR products, respectively. We thank David Schultz, Harry Whitmore, and Eric Taylor (The Jackson Laboratory) for colony management.

REFERENCES

1. Gordon, D. J., and B. M. Rifkind. 1989. High-density lipoprotein the clinical implications of recent studies. *N. Engl. J. Med.* **321:** 1311–1316.
2. Paigen, B., and M. C. Carey. 2002. Gallstones. *In* The Genetic Basis of Common Diseases. R. A. King, J. I. Rotter, and A. G. Motulsky, editors. Oxford University Press, New York. 298–335.
3. Tall, A. R., N. Wang, and P. Mucksavage. 2001. Is it time to modify the reverse cholesterol transport model? *J. Clin. Invest.* **108:** 1273–1275.
4. Osono, Y., L. A. Woollett, K. R. Marotti, G. W. Melchior, and J. M. Dietschy. 1996. Centripetal cholesterol flux from extrahepatic organs to the liver is independent of the concentration of high density lipoprotein-cholesterol in plasma. *Proc. Natl. Acad. Sci. USA.* **93:** 4114–4119.
5. Jolley, C. D., L. A. Woollett, S. D. Turley, and J. M. Dietschy. 1998. Centripetal cholesterol flux to the liver is dictated by events in the peripheral organs and not by the plasma high density lipoprotein or apolipoprotein A-I concentration. *J. Lipid Res.* **39:** 2143–2149.
6. Alam, K., R. S. Meidell, and D. K. Spady. 2001. Effect of up-regulating individual steps in the reverse cholesterol transport pathway on reverse cholesterol transport in normolipidemic mice. *J. Biol. Chem.* **276:** 15641–15649.
7. Blum, C. B., R. B. Dell, R. H. Palmer, R. Ramakrishnan, A. H. Seplowitz, and D. S. Goodman. 1985. Relationship of the parameters of body cholesterol metabolism with plasma levels of HDL cholesterol and the major HDL apoproteins. *J. Lipid Res.* **26:** 1079–1088.
8. van Eck, M., I. S. Bos, W. E. Kaminski, E. Orso, G. Rothe, J. Twisk, A. Bottcher, E. S. Van Amersfoort, T. A. Christiansen-Weber, W. P. Fung-Leung, T. J. Van Berkel, and G. Schmitz. 2002. Leukocyte ABCA1 controls susceptibility to atherosclerosis and macrophage recruitment into tissues. *Proc. Natl. Acad. Sci. USA.* **99:** 6298–6303.
9. Aiello, R. J., D. Brees, P. A. Bourassa, L. Royer, S. Lindsey, T. Coskran, M. Haghpassand, and O. L. Francone. 2002. Increased atherosclerosis in hyperlipidemic mice with inactivation of ABCA1 in macrophages. *Arterioscler. Thromb. Vasc. Biol.* **22:** 630–637.
10. Rust, S., M. Rosier, H. Funke, J. Real, Z. Amoura, J. C. Piette, J. F. Deleuze, H. B. Brewer, N. Duverger, P. Denefle, and G. Assmann. 1999. Tangier disease is caused by mutations in the gene encoding ATP-binding cassette transporter 1. *Nat. Genet.* **22:** 352–355.
11. Bodzioch, M., E. Orso, J. Klucken, T. Langmann, A. Bottcher, W. Diederich, W. Drobnik, S. Barlage, C. Buchler, M. Porsch-Ozcurumez, W. E. Kaminski, H. W. Hahmann, K. Oette, G. Rothe, C. Aslanidis, K. J. Lackner, and G. Schmitz. 1999. The gene encoding ATP-binding cassette transporter 1 is mutated in Tangier disease. *Nat. Genet.* **22:** 347–351.
12. Mertens, A., and P. Holvoet. 2001. Oxidized LDL and HDL: antagonists in atherothrombosis. *FASEB J.* **15:** 2073–2084.
13. Barter, P. J., P. W. Baker, and K. A. Rye. 2002. Effect of high-density lipoproteins on the expression of adhesion molecules in endothelial cells. *Curr. Opin. Lipidol.* **13:** 285–288.
14. Kannel, W. B., W. P. Castelli, and T. Gordon. 1979. Cholesterol in the prediction of atherosclerotic disease. New perspectives based on the Framingham study. *Ann. Intern. Med.* **90:** 85–91.
15. Calabresi, L., and G. Franceschini. 1997. High density lipoprotein and coronary heart disease: insights from mutations leading to low high density lipoprotein. *Curr. Opin. Lipidol.* **8:** 219–224.
16. Goldstein, J. L., and M. S. Brown. 2001. Molecular medicine. The cholesterol quartet. *Science.* **292:** 1310–1312.
17. Pullinger, C. R., C. Eng, G. Salen, S. Shefer, A. K. Batta, S. K. Erickson, A. Verhagen, C. R. Rivera, S. J. Mulvihill, M. J. Malloy, and J. P. Kane. 2002. Human cholesterol 7α-hydroxylase (CYP7A1) deficiency has a hypercholesterolemic phenotype. *J. Clin. Invest.* **110:** 109–117.
18. Wang, X., and B. Paigen. 2002. Quantitative trait loci and candidate genes regulating HDL cholesterol: a murine chromosome map. *Arterioscler. Thromb. Vasc. Biol.* **22:** 1390–1401.
19. Guttmacher, A. E., and F. S. Collins. 2002. Genomic medicine-a primer. *N. Engl. J. Med.* **347:** 1512–1520.
20. Lander, E. S., and D. Botstein. 1989. Mapping mendelian factors underlying quantitative traits using RFLP linkage maps. *Genetics.* **121:** 185–199.
21. Korstanje, R., and B. Paigen. 2002. From QTL to gene: the harvest begins. *Nat. Genet.* **31:** 235–236.
22. Khanuja, B., Y. C. Cheah, M. Hunt, P. M. Nishina, D. Q-H. Wang, H. W. Chen, J. T. Billheimer, M. C. Carey, and B. Paigen. 1995. *Lith1*, a major gene affecting cholesterol gallstone formation among inbred strains of mice. *Proc. Natl. Acad. Sci. USA.* **92:** 7729–7733.
23. Lammert, F., M. C. Carey, and B. Paigen. 2001. Chromosomal organization of candidate genes involved in cholesterol gallstone formation: a murine gallstone map. *Gastroenterology.* **120:** 221–238.
24. Lyons, M. A., H. Wittenburg, R. Li, R. Korstanje, K. Walsh, G. A. Churchill, M. C. Carey, and B. Paigen. 2003. *Lith6* encompasses PPARγ and SLC21A1 which are likely genetic determinants of murine cholesterol gallstone formation. In press.
25. Allain, C. C., L. S. Poon, C. S. Chan, W. Richmond, and P. C. Fu. 1974. Enzymatic determination of total serum cholesterol. *Clin. Chem.* **20:** 470–475.
26. Roeschlau, P., E. Bernt, and W. Gruber. 1974. Enzymatic determination of total cholesterol in serum. *Z. Klin. Chem. Klin. Biochem.* **12:** 226.
27. Warnick, G. R., C. Mayfield, J. Benderson, J. S. Chen, and J. J. Albers. 1982. HDL cholesterol quantitation by phosphotungstate-Mg^{2+} and by dextran sulfate-Mn^{2+}-polyethylene glycol precipitation, both with enzymic cholesterol assay compared with the lipid research method. *Am. J. Clin. Pathol.* **78:** 718–723.
28. de Faria, E., L. G. Fong, M. Komaromy, and A. D. Cooper. 1996. Relative roles of the LDL receptor, the LDL receptor-like protein, and hepatic lipase in chylomicron remnant removal by the liver. *J. Lipid Res.* **37:** 197–209.
29. Sen, S., and G. A. Churchill. 2001. A statistical framework for quantitative trait mapping. *Genetics.* **159:** 371–387.
30. Wittenburg, H., M. A. Lyons, R. Li, G. A. Churchill, M. C. Carey, and B. Paigen. 2003. Primary roles of FXR and ABCG5/ ABCG8 in cholesterol gallstone susceptibility: evidence from a cross of PERA/Ei and I/Ln inbred mice. In press.
31. Churchill, G. A., and R. W. Doerge. 1994. Empirical threshold values for quantitative trait mapping. *Genetics.* **138:** 963–971.
32. Paigen, B., D. Mitchell, K. Reue, A. Morrow, A. J. Lusis, and R. C. LeBoeuf. 1987. *Ath-1*, a gene determining atherosclerosis susceptibility and high density lipoprotein levels in mice. *Proc. Natl. Acad. Sci. USA.* **84:** 3763–3767.
33. Machleder, D., B. Ivandic, C. Welch, L. Castellani, K. Reue, and A. J. Lusis. 1997. Complex genetic control of HDL levels in mice in response to an atherogenic diet. Coordinate regulation of HDL levels and bile acid metabolism. *J. Clin. Invest.* **99:** 1406–1419.
34. Srivastava, R. A. K., N. Srivastava, and M. Averna. 2000. Dietary cholic acid lowers plasma levels of mouse and human apolipoprotein A-I primarily via a transcriptional mechanism. *Eur. J. Biochem.* **267:** 4272–4280.
35. Moore, K. J., and D. L. Nagle. 2000. Complex trait analysis in the mouse: The strengths, the limitations and the promise yet to come. *Annu. Rev. Genet.* **34:** 653–686.
36. Mehrabian, M., L. W. Castellani, P. Z. Wen, J. Wong, T. Rithaporn, S. Y. Hama, G. P. Hough, D. Johnson, J. J. Albers, G. A. Mottino, J. S. Frank, M. Navab, A. M. Fogelman, and A. J. Lusis. 2000. Genetic control of HDL levels and composition in an interspecific mouse cross (CAST/Ei × C57BL/6J). *J. Lipid Res.* **41:** 1936–1946.

37. Tsipouri, V., J. A. Curtin, T. A. Hough, P. M. Nolan, L. J. Rooke, L. Vizor, J. Peters, A. J. Hunter, D. Rogers, S. Rastan, J. Martin, S. D. Brown, E. M. Fisher, N. K. Spurr, and I. C. Grey. 2001. Mapping an ENU mutagenesis derived, low total cholesterol, low HDL-cholesterol mutant mouse to chromosome 4. *In* MGI Direct Data Submission, http://www.informatics.jax.org/searches/allele.cgi?3736 Bar Harbor, ME. Accepted 20 March 2003.
38. Arya, R., R. Duggirala, L. Almasy, D. L. Rainwater, M. C. Mahaney, S. Cole, T. D. Dyer, K. Williams, R. J. Leach, J. E. Hixson, J. W. MacCluer, P. O'Connell, M. P. Stern, and J. Blangero. 2002. Linkage of high-density lipoprotein-cholesterol concentrations to a locus on chromosome 9p in Mexican Americans. *Nat. Genet.* **30:** 102–105.
39. Ober, C., M. Abney, and M. S. McPeek. 2001. The genetic dissection of complex traits in a founder population. *Am. J. Hum. Genet.* **69:** 1068–1079.
40. Ishibashi, S., M. S. Brown, J. L. Goldstein, R. D. Gerard, R. E. Hammer, and J. Herz. 1993. Hypercholesterolemia in low density lipoprotein receptor knockout mice and its reversal by adenovirus-mediated gene delivery. *J. Clin. Invest.* **92:** 883–893.
41. Hofmann, S. L., D. W. Russell, M. S. Brown, J. L. Goldstein, and R. E. Hammer. 1988. Overexpression of low density lipoprotein (LDL) receptor eliminates LDL from plasma in transgenic mice. *Science.* **239:** 1277–1281.
42. Yokode, M., R. E. Hammer, S. Ishibashi, M. S. Brown, and J. L. Goldstein. 1990. Diet-induced hypercholesterolemia in mice: prevention by overexpression of LDL receptors. *Science.* **250:** 1273–1275.
43. Orso, E., C. Broccardo, W. E. Kaminski, A. Bottcher, G. Liebisch, W. Drobnik, A. Gotz, O. Chambenoit, W. Diederich, T. Langmann, T. Spruss, M. F. Luciani, G. Rothe, K. J. Lackner, G. Chimini, and G. Schmitz. 2000. Transport of lipids from Golgi to plasma membrane is defective in Tangier disease patients and Abc1-deficient mice. *Nat. Genet.* **24:** 192–196.
44. Christiansen-Weber, T. A., J. R. Voland, Y. Wu, K. Ngo, B. L. Roland, S. Nguyen, P. A. Peterson, and W-P. Fung-Leung. 2000. Functional loss of ABCA1 in mice causes severe placental malformation, aberrant lipid distribution, and kidney glomerulonephritis as well as high-density lipoprotein cholesterol deficiency. *Am. J. Pathol.* **157:** 1017–1029.
45. McNeish, J., R. J. Aiello, D. Guyot, T. Turi, C. Gabel, C. Aldinger, K. L. Hoppe, M. L. Roach, L. J. Royer, J. de Wet, C. Broccardo, G. Chimini, and O. L. Francone. 2000. High density lipoprotein deficiency and foam cell accumulation in mice with targeted disruption of ATP-binding cassette transporter-1. *Proc. Natl. Acad. Sci. USA.* **97:** 4245–4250.
46. Vaisman, B. L., G. Lambert, M. Amar, C. Joyce, T. Ito, R. D. Shamburek, W. J. Cain, J. Fruchart-Najib, E. D. Neufeld, A. T. Remaley, H. B. Brewer, Jr., and S. Santamarina-Fojo. 2001. ABCA1 overexpression leads to hyperalphalipoproteinemia and increased biliary cholesterol excretion in transgenic mice. *J. Clin. Invest.* **108:** 303–309.
47. Singaraja, R. R., V. Bocher, E. R. James, S. M. Clee, L-H. Zhang, B. R. Leavitt, B. Tan, A. Brooks-Wilson, A. Kwok, N. Bissada, Y-z. Yang, G. Liu, S. R. Tafuri, C. Fievet, C. L. Wellington, B. Staels, and M. R. Hayden. 2001. Human ABCA1 BAC transgenic mice show increased high density lipoprotein cholesterol and ApoAI-dependent efflux stimulated by an internal promoter containing liver X receptor response elements in intron 1. *J. Biol. Chem.* **276:** 33969–33979.
48. Mehrabian, M., P. Z. Wen, J. Fisler, R. C. Davis, and A. J. Lusis. 1998. Genetic loci controlling body fat, lipoprotein metabolism, and insulin levels in a multifactorial mouse model. *J. Clin. Invest.* **101:** 2485–2496.
49. Nishina, P. M., S. Lowe, J. Wang, and B. Paigen. 1994. Characterization of plasma lipids in genetically obese mice: the mutants obese, diabetes, fat, tubby, and lethal yellow. *Metabolism.* **43:** 549–553.
50. Lutucuta, S., C. M. Ballantyne, H. Elghannam, A. M. Gotto, Jr., and A. J. Marian. 2001. Novel polymorphisms in promoter region of ATP binding cassette transporter gene and plasma lipids, severity, progression, and regression of coronary atherosclerosis and response to therapy. *Circ. Res.* **88:** 969–973.
51. Hammad, S. M., J. L. Barth, C. Knaak, and W. S. Argraves. 2000. Megalin acts in concert with cubilin to mediate endocytosis of high density lipoproteins. *J. Biol. Chem.* **275:** 12003–12008.
52. Christensen, E. I., and H. Birn. 2002. Megalin and cubilin: multifunctional endocytic receptors. *Nat. Rev. Mol. Cell Biol.* **3:** 256–266.
53. Willnow, T. E., J. Hilpert, S. A. Armstrong, A. Rohlmann, R. E. Hammer, D. K. Burns, and J. Herz. 1996. Defective forebrain development in mice lacking gp330/megalin. *Proc. Natl. Acad. Sci. USA.* **93:** 8460–8464.
54. Edwards, P. A., H. R. Kast, and A. M. Anisfeld. 2002. BAREing it all. The adoption of LXR and FXR and their roles in lipid homeostasis. *J. Lipid Res.* **43:** 2–12.
55. Peet, D. J., S. D. Turley, W. Ma, B. A. Janowski, J. M. Lobaccaro, R. E. Hammer, and D. J. Mangelsdorf. 1998. Cholesterol and bile acid metabolism are impaired in mice lacking the nuclear oxysterol receptor LXR alpha. *Cell.* **93:** 693–704.
56. Alberti, S., G. Schuster, P. Parini, D. Feltkamp, U. Diczfalusy, M. Rudling, B. Angelin, I. Bjorkhem, S. Pettersson, and J-A. Gustafsson. 2001. Hepatic cholesterol metabolism and resistance to dietary cholesterol in LXRβ-deficient mice. *J. Clin. Invest.* **107:** 565–573.
57. Boelsterli, U. A., and M. Bedoucha. 2002. Toxicological consequences of altered peroxisome proliferator-activated receptor gamma (PPARgamma) expression in the liver: insights from models of obesity and type 2 diabetes. *Biochem. Pharmacol.* **63:** 1–10.
58. Barak, Y., M. C. Nelson, E. S. Ong, Y. Z. Jones, P. Ruiz-Lozano, K. R. Chien, A. Koder, and R. M. Evans. 1999. PPAR gamma is required for placental, cardiac, and adipose tissue development. *Mol. Cell.* **4:** 585–595.
59. Li, A. C., K. K. Brown, M. J. Silvestre, T. M. Willson, W. Palinski, and C. K. Glass. 2000. Peroxisome proliferator-activated receptor γ ligands inhibit development of atherosclerosis in LDL receptor-deficient mice. *J. Clin. Invest.* **106:** 523–531.
60. Miles, P. D. G., Y. Barak, W. He, R. M. Evans, and J. M. Olefsky. 2000. Improved insulin-sensitivity in mice heterozygous for PPARγ deficiency. *J. Clin. Invest.* **105:** 287–292.
61. Walczak, R., and P. Tontonoz. 2002. PPARadigms and PPARadoxes: expanding roles for PPARγ in the control of lipid metabolism. *J. Lipid Res.* **43:** 177–186.
62. Hirano, K-I., S. G. Young, R. V. Farese, Jr., J. Ng, E. Sande, C. Warburton, L. M. Powell-Braxton, and N. O. Davidson. 1996. Targeted disruption of the mouse Apobec-1 gene abolishes apolipoprotein B mRNA editing and eliminates apolipoprotein B48. *J. Biol. Chem.* **271:** 9887–9890.
63. Mehrabian, M., J. Wong, X. Wang, Z. Jiang, W. Shi, A. M. Fogelman, and A. J. Lusis. 2001. Genetic locus in mice that blocks development of atherosclerosis despite extreme hyperlipidemia. *Circ. Res.* **89:** 125–130.
64. Nakamuta, M., B. H. Chang, E. Zsigmond, K. Kobayashi, H. Lei, B. Y. Ishida, K. Oka, E. Li, and L. Chan. 1996. Complete phenotypic characterization of apobec-1 knockout mice with a wild-type genetic background and a human apolipoprotein B transgenic background, and restoration of apolipoprotein B mRNA editing by somatic gene transfer of Apobec-1. *J. Biol. Chem.* **271:** 25981–25988.
65. Morrison, J. R., C. Paszty, M. E. Stevens, S. D. Hughes, T. Forte, J. Scott, and E. M. Rubin. 1996. Apolipoprotein B RNA editing enzyme-deficient mice are viable despite alterations in lipoprotein metabolism. *Proc. Natl. Acad. Sci. USA.* **93:** 7154–7159.
66. Nakamuta, M., S. Taniguchi, B. Y. Ishida, K. Kobayashi, and L. Chan. 1998. Phenotype interaction of *apobec-1* and *CETP*, *LDLR*, and *ApoE* gene expression in mice: role of ApoB mRNA editing in lipoprotein phenotype expression. *Arterioscler. Thromb. Vasc. Biol.* **18:** 747–755.
67. Teng, B., S. Blumenthal, T. Forte, N. Navaratnam, J. Scott, A. M. Gotto, Jr., and L. Chan. 1994. Adenovirus-mediated gene transfer of rat apolipoprotein B mRNA-editing protein in mice virtually eliminates apolipoprotein B-100 and normal low density lipoprotein production. *J. Biol. Chem.* **269:** 29395–29404.
68. Yamanaka, S., M. Balestra, L. Ferrell, J. Fan, K. Arnold, S. Taylor, J. Taylor, and T. Innerarity. 1995. Apolipoprotein B mRNA-editing protein induces hepatocellular carcinoma and dysplasia in transgenic animals. *Proc. Natl. Acad. Sci. USA.* **92:** 8483–8487.
69. Teng, B., B. Ishida, T. M. Forte, S. Blumenthal, L. Z. Song, A. M. Gotto, Jr., and L. Chan. 1997. Effective lowering of plasma, LDL, and esterified cholesterol in LDL receptor-knockout mice by adenovirus-mediated gene delivery of ApoB mRNA editing enzyme (*Apobec1*). *Arterioscler. Thromb. Vasc. Biol.* **17:** 889–897.
70. Qian, X., M. E. Balestra, S. Yamanaka, J. Boren, I. Lee, and T. L. Innerarity. 1998. Low expression of the apolipoprotein B mRNA-editing transgene in mice reduces LDL levels but does not cause liver dysplasia or tumors. *Arterioscler. Thromb. Vasc. Biol.* **18:** 1013–1020.
71. Chawla, A., W. A. Boisvert, C. H. Lee, B. A. Laffitte, Y. Barak, S. B.

Joseph, D. Liao, L. Nagy, P. A. Edwards, L. K. Curtiss, R. M. Evans, and P. Tontonoz. 2001. A PPAR gamma-LXR-ABCA1 pathway in macrophages is involved in cholesterol efflux and atherogenesis. *Mol. Cell.* **7:** 161–171.

72. Haghpassand, M., P. A. Bourassa, O. L. Francone, and R. J. Aiello. 2001. Monocyte/macrophage expression of ABCA1 has minimal contribution to plasma HDL levels. *J. Clin. Invest.* **108:** 1315–1320.
73. Krimbou, L., M. Marcil, J. Davignon, and J. Genest, Jr. 2001. Interaction of lecithin:cholesterol acyltransferase (LCAT).α_2-macroglobulin complex with low density lipoprotein receptor-related protein (LRP). Evidence for an α_2-macroglobulin/LRP receptor-mediated system participating in LCAT clearance. *J. Biol. Chem.* **276:** 33241–33248.
74. Umans, L., L. Serneels, L. Overbergh, K. Lorent, F. Van Leuven, and H. Van den Berghe. 1995. Targeted inactivation of the mouse alpha 2-macroglobulin gene. *J. Biol. Chem.* **270:** 19778–19785.
75. Pinson, K. I., J. Brennan, S. Monkley, B. J. Avery, and W. C. Skarnes. 2000. An LDL-receptor-related protein mediates *Wnt* signalling in mice. *Nature.* **407:** 535–538.
76. Welch, C. L., S. Bretschger, N. Latib, M. Bezouevski, Y. Guo, N. Pleskac, C-P. Liang, C. Barlow, H. Dansky, J. L. Breslow, and A. R. Tall. 2001. Localization of atherosclerosis susceptibility loci to chromosomes 4 and 6 using the *Ldlr* knockout mouse model. *Proc. Natl. Acad. Sci. USA.* **98:** 7946–7951.
77. Drake, T. A., E. Schadt, K. Hannani, J. M. Kabo, K. Krass, V. Colinayo, L. E. Greaser 3rd, J. Goldin, and A. J. Lusis. 2001. Genetic loci determining bone density in mice with diet-induced atherosclerosis. *Physiol. Genomics.* **5:** 205–215.
78. Oka, K., K. Kobayashi, M. Sullivan, J. Martinez, B-B. Teng, K. Ishimura-Oka, and L. Chan. 1997. Tissue-specific inhibition of apolipoprotein B mRNA editing in the liver by adenovirus-mediated transfer of a dominant negative mutant APOBEC-1 leads to increased low density lipoprotein in mice. *J. Biol. Chem.* **272:** 1456–1460.